Spiral Computed Tomographic Imaging Related to Computerized Ultrasonographic Images of Carotid Plaque Morphology and Histology

Marie-Louise M. Grønholdt, MD, PhD, Aase Wagner, MD, Britt M. Wiebe, MD, Jon U. Hansen, MSEE, Torben V. Schroeder, MD, DMSc, Jens E. Wilhjelm, MSEE, PhD, Markus Nowak, MSc, Henrik Sillesen, MD, DMSc

Objective. Echolucency of carotid atherosclerotic plaques, as evaluated by computerized B-mode ultrasonographic images, has been associated with an increased incidence of brain infarcts on cerebral computed tomographic scans. We tested the hypotheses that characterization of carotid plaques on spiral computed tomographic images correlates with that on computerized B-mode ultrasonographic images and that spiral computed tomographic imaging predicts the histomorphometric plaque content. ***Methods.*** The study included 38 patients with neurologic symptoms and at least 50% stenosis of the ipsilateral carotid artery. High-resolution B-mode ultrasonographic images and spiral computed tomographic images of carotid plaques were computer processed to yield a quantitative measure, the gray scale level of the plaque. ***Results.*** The mean Hounsfield value for spiral computed tomographic images correlated with the gray scale median for B-mode ultrasonographic images (univariate linear regression analysis: r = 0.45; P = .01) and the histologic content of calcification in the plaque (r = 0.34; P = .04) but not with lipid, hemorrhage, or fibrous tissue in the plaque. ***Conclusions***. Spiral computed tomographic imaging seems to correlate with B-mode ultrasonographic imaging for showing plaque characteristics. Spiral computed tomographic attenuation was also correlated with the amount of calcification noted on histologic examination but not with lipid and hemorrhage, the components thought to characterize vulnerable, rupture-prone plaques. Key words: arteriosclerosis; carotid artery disease; tomography; ultrasonography; histology.

Abbreviations
CI, confidence interval; CT, computed tomographic

Received October 17, 2000, from the Departments of Vascular Surgery (M.-L.M.G., T.V.S.), and Neuroradiology (A.W.), Laboratory of Neuropathology (B.M.W.), and Center for Imaging, Informatics and Engineering in Medicine (M.N.), Rigshospitalet, Copenhagen, Denmark; Department of Information Technology, Technical University of Denmark, Lyngby, Denmark (J.U.H., J.E.W.); and Department of Vascular Surgery, Gentofte Hospital, Hellerup, Denmark (H.S.). Revision requested November 21, 2000. Revised manuscript accepted for publication January 9, 2001.

This work was supported by Hjernesagen and the Danish Medical and Technical Research Council under the Center for Arteriosclerosis Detection by Ultrasound.

Address correspondence and reprint requests to Marie-Louise M. Grønholdt, MD, PhD, Blomstervaenget 18, 2800 Lyngby, Denmark.

At present, the indication for carotid surgery is based on clinical evaluation and the degree of stenosis, measured by Doppler ultrasonography, digital subtraction angiography, and computed tomographic (CT) or magnetic resonance angiography.[1] European and North American carotid surgery trials have shown the benefit of carotid endarterectomy in patients with angiographically detected symptomatic carotid stenosis of 70% or greater.[2,3] However, studies on both the carotid and coronary arteries suggest that many events (approximately 50%) are attributable to plaques in these arteries narrowing the lumen by 50% or less, suggesting that plaque rupture is an important causative mechanism.[4] Moreover, recent publications have indicated that the imaged morphology and histologic content of the carotid artery plaque, as well as cardiovascular risk fac-

tors, may also influence the prognosis and therefore the indication for intervention.[5]

With the use of B-mode ultrasonographic imaging, vulnerable and rupture-prone carotid plaques causing cerebrovascular symptoms and infarctions have been subjectively characterized as echolucent and heterogeneous and objectively (computer-assisted) characterized as having a low gray scale value.[5,6] Histologically, vulnerable carotid plaques have a lipid-rich necrotic core covered by a thin, rupture-prone fibrous cap and signs of ongoing inflammation, because they are heavily infiltrated by macrophages.[7,8] Magnetic resonance imaging may be a good discriminator of vulnerable carotid plaque features in vitro and probably also in vivo.[9–11] Whereas carotid plaque stenosis and morphology have been evaluated by B-mode ultrasonographic imaging for more than a decade, conventional angiography has mostly been abandoned, because it has a morbidity risk of about 1%, cannot distinguish morphologic features (including ulcerated surfaces[12]), and is more expensive and invasive than duplex ultrasonography.[13] In light of the facts that the relationship of ultrasonography to the standard of reference, histopathologic examination, has never been satisfactory[1,5] and that magnetic resonance imaging still is evolving for characterization in vivo, the search for other modalities for prediction of vulnerable carotid plaques has been continuous. To our knowledge, very few studies have tested the ability of spiral CT imaging[14,15] to evaluate plaque morphology. The aim of this study, therefore, was to investigate a possible correlation between spiral CT and ultrasonographic evaluation of carotid plaque morphology and to compare the abilities of these 2 methods to predict the histologic plaque composition.

Materials and Methods

Materials

Thirty-eight consecutive patients (22 men and 16 women; median age, 60 years) undergoing carotid endarterectomy were prospectively enrolled. All patients had experienced neurologic symptoms relevant to a carotid stenosis of 50% or greater as proved by duplex ultrasonography. Symptoms were stroke (n = 18 [47%]), transient ischemic attack (n = 12 [32%]), and amaurosis fugax (n = 8 [21%]). Before carotid endarterectomy, all patients underwent B-mode ultrasonographic scanning and spiral CT imaging for evaluation of carotid plaque morphology. The study was approved by the medical ethics committee for Copenhagen and Frederiksberg counties (KF 01-375/94), and all patients gave informed consent.

Spiral CT Imaging

CT imaging was performed with a General Electric Prospeed VX scanner (GE Medical Systems, Waukesha, WI). The bifurcation level of the relevant carotid artery was identified on a scout localization image. After that, a spiral scan located around the mean level of the bifurcation was performed (2-mm/s table speed, 2-mm pitch, 120 kV, 160 mA, 1.5-second scan time, and 50 mL of contrast media intravenously injected by pump injector at 3 mL/s, performing the scan after a 20-second delay, covering a total of 6 cm). A total of 30 images with contrast in the lumen were reconstructed with a 2-mm increment interval (Fig. 1). After transferring data (digitized in 12 bits) from the scanner to a Siemens Magic View workstation (Siemens Medical Systems, Issaquah, WA), images were converted from a three-dimensional spiral format to a two-dimensional format for later digital analysis.

The region of interest covering 6 cm around the bifurcation of the carotid artery included the distal part of the common carotid artery, the bifurcation, and the proximal part of the internal carotid artery. These parts of the artery were marked on hard copies on the 30 corresponding spiral CT images with luminal contrast by an experienced neuroradiologist (A.W.), who was unaware of the ultrasonographic and histologic results. Outlines on the 30 digital images per patient were drawn (J.U.H.) under guidance of the marked hard copies (A.W.). Specifically, 1 (inner) outline of the residual lumen

Figure 1. (facing page) Characteristics of a calcified and lipid-rich carotid plaque on the 3 different imaging modalities. **A**, High-density calcified plaque: spiral CT imaging in a cross-sectional plane. **B**, Echo-rich acoustic shadowing: B-mode ultrasonographic imaging in the longitudinal plane. **C**, Histologic staining (hematoxylin-eosin) of the plaque, cut in a cross-sectional plane. **D–F**, Longitudinal images of a lipid-rich, low-density, echolucent plaque. Next to the total spiral CT image (**D**, top left), the relevant cross-sectional section with the right carotid artery is enlarged (with luminal contrast). To show the outlines of the echolucent plaque, the corresponding color Doppler image was placed under the B-mode image. C indicates calcification in the plaque; CCA, common carotid artery; ICA, internal carotid artery; F, fibrous tissue; and L, lipid. On the ultrasonographic images, the original distance between the dots on right scale was 2 mm. Original magnification of histologic images ×20.

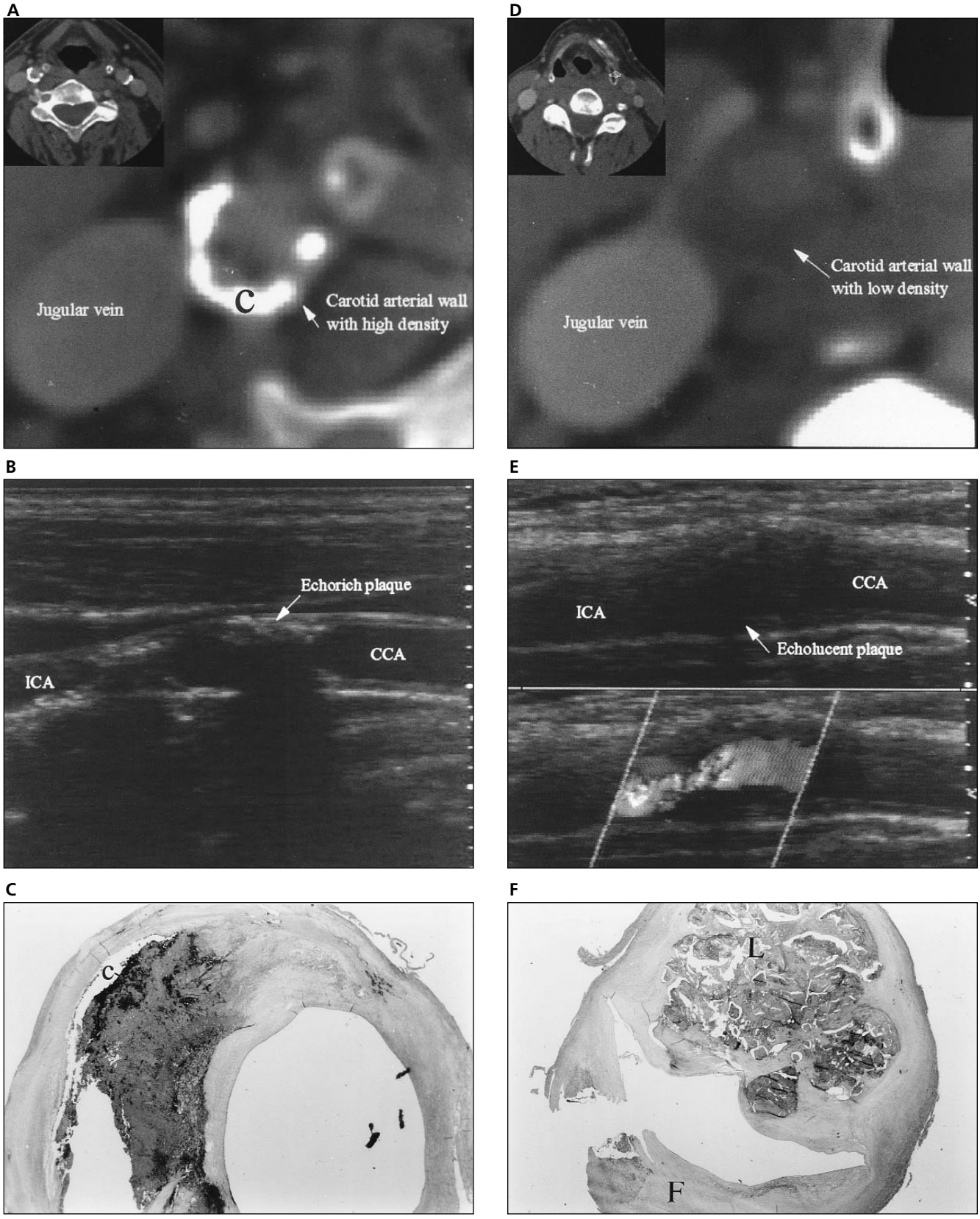
A
Jugular vein
C
Carotid arterial wall
with high density
D
Carotid arterial wall
with low density
Jugular vein
B
Echorich plaque
CCA
ICA
E
CCA
ICA
Echolucent plaque
C
C
F
L
F

and 1 (outer) following the arterial wall were drawn on each CT image. In a gross magnification, the drawing of the inner outline was easier. Hence, the plaque and arterial wall could be distinguished from the luminal contrast, depicted as confluent monochromatic pixels. The region between these 2 outlines corresponded to the plaque and arterial wall. The mean attenuation value of the plaque (and arterial wall) in Hounsfield units was finally calculated for this region, as well as a mean value for each patient, averaging all 30 images. Variability of the CT image analysis was tested by the same observer (J.U.H., intraobserver) and a second observer (M.-L.M.G., interobserver), both redrawing outlines on the 30 digital CT images from 5 randomly chosen patients.

Ultrasonographic Examination

Carotid ultrasonographic scanning was performed with an Interspec RX 400 system (ATL Ultrasound, Bothell, WA) with a 5- to 10-MHz linear array transducer. Fixed settings of maximum dynamic range, a high frame rate, and a linear postprocessing curve were used for each scan. Time-gain compensation curves were gently sloped, except for being vertical in the arterial lumen to obtain the same echogenicity of the near and far arterial walls. At the beginning of each ultrasonographic examination, the gain was set to the point at which blood appeared black (free of noise). The degree of stenosis was determined by using Doppler criteria in which 120-cm/s systolic velocity equaled 50% stenosis and 135-cm/s diastolic velocity equaled stenosis exceeding 80%. The median degree of stenosis was 80% (range, 50%–95%). Furthermore, the best available high-resolution B-mode and color Doppler images of the plaque from a scan plane lateral to the sternocleidomastoid muscle and longitudinal to the vessel were recorded on videotape and later digitized off-line on a personal computer using a Targa 2000-E frame grabber (Truevision Inc, Indianapolis, IN; Fig. 1). All ultrasonographic images were centered around the bifurcation for later comparison with the CT images, aligned in the same manner.

The B-mode and corresponding color Doppler images were processed with the software program Image-Pro Plus, version 1.2.01 for Windows (Media Cybernetics, Silver Spring, MD). The carotid artery plaque was outlined on the B-mode image, and the gray scale values of all pixels within this outlined region were used to generate a median gray scale value (0–255; 0 = black and 255 = white); in cases of acoustic shadowing from a plaque, the outline did not include this shadow region. To standardize the images for the echogenicity of blood, an area of blood was also outlined on the B-mode ultrasonographic image for each patient. A standardized gray scale value was calculated as the difference in mean gray scale level between the region of the atherosclerotic plaque and blood. Ultrasonographic examinations and generation of outlines were all performed by a single experienced ultrasonographer (M.-L.M.G.), unaware of the results from the spiral CT imaging and the histologic examination.

Histologic Examination

The carotid artery plaques were removed in toto during endarterectomy (T.V.S.). After the external carotid artery was discarded, the remaining plaque was cut transversely into 3-mm-thick blocks (4–14 blocks per patient). Consecutive sections from each block were stained with hematoxylin-eosin, van Gieson's, and Verhoeff's stains, respectively (Fig. 1). Plaque constituents (lipid, hemorrhage, calcification, thrombus, and fibrous tissue) in all sections were measured morphometrically by a single experienced pathologist (B.M.W.), using a Leitz (Cambridge, United Kingdom) Texture Analyzing System.[16] From the results of all sections, the total percentage of each constituent was calculated. The pathologist was unaware of results from the ultrasonographic examination and spiral CT imaging.

Statistical Analysis

Spearman rank correlations and multiple linear regressions were performed with the Statistica program (Statsoft, Tulsa, OK). To obtain a normal distribution, medians of ultrasonographic gray scale values, plaque calcification, and hemorrhage were transformed logarithmically before performance of stepwise multiple linear regression analysis of ultrasonographic and spiral CT values to find the best predictor of the histologic measurements. Reproducibility was tested using the method of Bland and Altman,[17] in which the difference between 2 repeated measurements was plotted against the mean of the same 2 measurements to calculate a mean bias and 95% confidence interval (CI). A coefficient of variation based on duplicate measurements was also calculated. $P \leq .05$ on 2-sided tests was considered statistically significant.

Results

Spiral CT and Ultrasonographic Plaque Morphology

Plaque morphology on spiral CT images (mean Hounsfield units) correlated significantly with morphology on B-mode ultrasonographic images (median gray scale levels, $r = 0.44$; $P = .01$; Fig. 2). The main results were the same whether unadjusted or adjusted gray scale levels of the ultrasonographic images were used or the outlier in Figure 2 was removed.

Spiral CT and Ultrasonography Versus Histologic Plaque Content

High values of mean Hounsfield units on spiral CT images were associated with a high content of calcification in the plaque, whereas there was no association with other plaque constituents (Table 1).

Although not significantly, the gray scale median level was negatively correlated to the relative plaque lipid and hemorrhage content and positively correlated to calcification and fibrous tissue content (Table 1). In a step-up multiple linear regression analysis, ultrasonography was found to be a better predictor than spiral CT imaging of all measured plaque constituents except for calcification (Table 2).

Age was positively associated with mean Hounsfield units on spiral CT imaging ($r = 0.40$; $P = .01$) and the gray scale median on B-mode ultrasonographic imaging ($r = 0.34$; $P = .04$).

Reproducibility

Intraobserver and interobserver variabilities of spiral CT measurements were calculated as mean bias of –4.3 (95% CI, –6.4 to –2.1) and +11.6 (95% CI, +7.8 to +15.5) and coefficients of variation of 9.9% and 17.2%, respectively. The Bland-Altman plots (Fig. 3A) of the intraobserver analysis clearly show that the repeated measurements are equally distributed around 0 (not biased). The interobserver plot (Fig. 3B) is skewed, with most values greater than 0, indicating a bias.

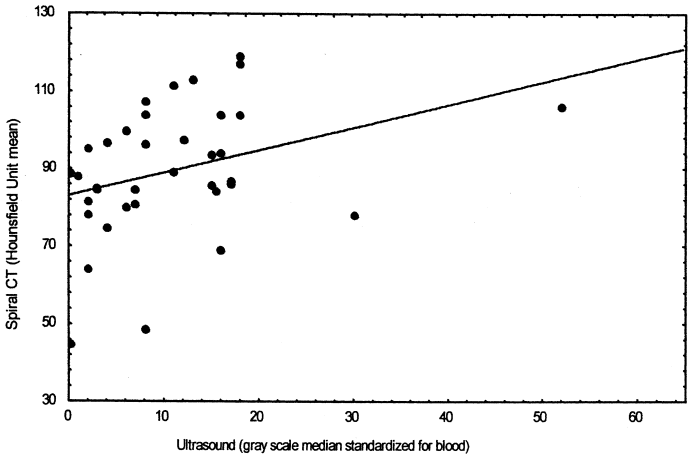

Figure 2. Scatter plot of plaque morphology on B-mode ultrasonographic images (median gray scale levels) plotted against spiral CT images (mean Hounsfield units).

Discussion

Previously, spiral CT imaging of carotid plaque morphology had only been related to histopathologic measurements of a few randomly chosen sections of the plaque, but it had not been related to the whole plaque. Neither had carotid plaque characterization using spiral CT imaging been correlated with B-mode ultrasonographic imaging. This is probably because of the workload required to gain and analyze data from the CT scanner for a whole plaque.

In a sample of 9 patients, Oliver et al[14] found that hypodense areas on CT imaging correlated with necrotic lipid debris, and isodense areas correlated with fibrosis on histologic evaluation. However, in 9 of 16 sections with an indication of calcifications on CT, this constituent was not found in the histologic evaluation. Furthermore, CT was a poor predictor of plaque ulceration, thickness of the fibrous cap, and plaque inflammation.[14] Unfortunately, there were several limitations: (1) the sample size was small; (2) only hard copy CT images were used; and (3) 3-mm-thick CT sections were correlated to some ran-

Table 1. Plaque Morphology Evaluated on Spiral CT Images and Correlated With the Corresponding Histologic Content in a Spearman Rank Correlation

Dependent Variable*	Spiral CT Mean		Ultrasound Gray Scale Median†	
	r	*P*	*r*	*P*
% plaque lipid (45%)	–0.14	.39	–0.31	.06
% plaque hemorrhage (0.4%)	–0.10	.57	–0.31	.07
% plaque calcification (0.8%)	0.34	.04	0.30	.07
% plaque fibrous tissue (54%)	0.09	.57	0.28	.09

The mean relative percentage of each plaque constituent is given in parentheses.
*Independent variable: histologic measurements.
†Standardized for blood.

Table 2. Ranking by Multiple Linear Regression Analysis of Spiral CT and B-Mode Ultrasonographic Images as Predictors of Histologic Content of Plaque Lipid, Hemorrhage, Calcification, and Fibrous Tissue in Carotid Plaques

Independent Variable	Rank	Multiple R^2	R^2 Change	*P*
% plaque lipid*				
Ultrasonographic gray scale median	1	0.11	0.11	.047
% plaque hemorrhage*				
Ultrasonographic gray scale median	1	0.08	0.08	.10
% plaque calcification*				
Spiral CT mean	1	0.08	0.08	.10
Ultrasonographic gray scale median	2	0.11	0.03	.28
% Plaque fibrous tissue*				
Ultrasonographic gray scale median	1	0.05	0.05	.19

*Dependent variable: histologic measurements.

domly chosen 5-µm histologic sections with a variable distance to the sole fix point (the bifurcation), without taking plaque shrinkage during pathologic preparation into consideration.

In a study of 21 asymptomatic and symptomatic patients with carotid plaque, Estes et al[15] found that CT imaging could qualitatively define plaque features containing calcium, fibrous stroma, and lipid. Furthermore, CT attenuation values could distinguish between lipid and fibrous stroma ($P < .001$) in a quantitative analysis.[15] Limitations in the latter study related to a questionable alignment of histologic and CT sections for correlation without accounting for shrinkage of the plaque.[15] The main results of the 2 studies[14,15] regarding the CT prediction of histologic content could not be reproduced in our more quantitative analysis on a relatively larger sample of symptomatic patients,[18] probably because of methodological variations among the 3 studies.

The present study and the 2 other studies discussed above are limited by problems of outlining the carotid plaque on the CT images. Flecks of calcium may result in inaccuracies in the delineation of the vessel lumen by blending with the contrast column in the lumen.[19] Furthermore, if the amount of contrast agent used is insufficient and the contrast agent bolus timing is not precise, maximal opacity of the carotid artery at the time of scanning is not obtained.[19] This would result in incorrect delineation of a plaque, also including the luminal area. However, the inner outline was easily detected in this study. The outer outline was found to be the most difficult to identify, and it introduced an interobserver bias (Fig. 3).

The measured length of carotid plaques could vary with the respective methods, CT imaging and histologic evaluation: (1) CT images of both the plaque and the entire arterial wall are always taken 3 cm below and above the bifurcation; and (2) at histologic evaluation the length of the plaque depends on the surgeon. Longitudinal plaque shrinkage after the histologic procedure

Figure 3. Bland-Altman plots showing the intraobserver (**A**) and interobserver (**B**) variability.[17] The mean value of the 2 sets of mean Hounsfield units from 150 spiral CT images is plotted on the x-axis. The difference between the 2 sets of measurements is plotted on the y-axis. On both plots, the differences are related to the size of the gray scale level. The dotted line indicates 2 SD, representing 95% of the observations.

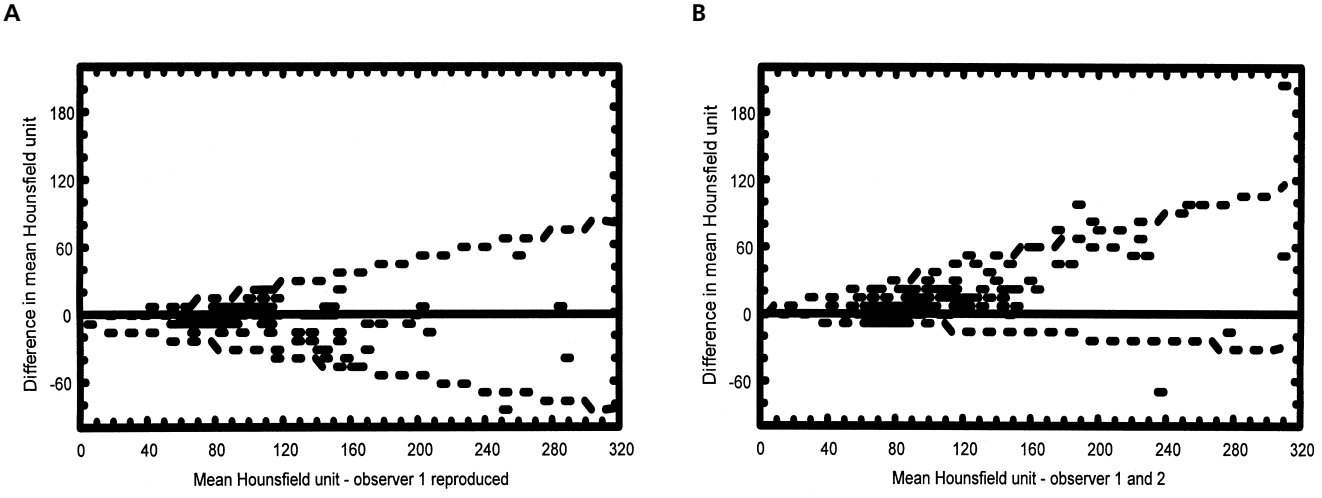

was probably a minor problem in this study, in which a correlation was done using the entire plaque. Using the entire plaque also reduces problems with correlating a longitudinal ultrasonographic image (plaque and part of the arterial media) in 2 dimensions with cross-sectional two-dimensional spiral CT images (plaque and the entire arterial wall) and histologic sections (plaque and part of the arterial media) in 3 dimensions (Fig. 1).[20] However, allowance for the possibility that the various plaque components can shrink differently was not done. Nevertheless, the reproducibility of the spiral CT method was acceptable, because the manual drawing of outlines on the spiral CT images was expected to be the most observer-dependent part of the investigation, introducing a bias. Compared with the fine accuracy of measuring the degree of stenosis on Doppler ultrasonography, subjective plaque evaluation by using B-mode ultrasonographic imaging is known to be very observer dependent and less accurate.[5] However, when a single sonographer (M.-L.M.G.) performed the less-observer-dependent computer-assisted plaque evaluation, the intraobserver variability was low (mean bias, –0.4; 95% CI, –1.5 to +0.1; coefficient of variation, 5.5%).[18] Likewise, the mean biases for histologic examination of relative plaque lipid and fibrous tissue content were acceptable: +0.6% (95% CI, –1.5% to +2.6%) and +1.1% (95% CI, –0.8% to +3.1%); coefficients of variation, 3.5%, and 2.2%, respectively.[16]

B-mode ultrasonographic imaging is a noninvasive method for investigating plaque morphology, but it has limitations, such as acoustic shadowing attributable to calcifications in the plaque, speckle diffraction, and angle dependence.[20,21] In the present study, the ultrasonographically measured gray scale level had a correlation coefficient identical to those of plaque lipid and fibrous tissue content (Table 2), as for a larger sample reported previously, in which these correlations were significant.[18] Despite the general finding that ultrasonographic features relate to histologic components, prediction of plaque components from ultrasonography for a single patient is not possible. Compared with ultrasonography, on CT imaging calcification does not obscure a part of the image, allowing quantification of the amount and volume of plaque calcium in coronary plaques.[22–24] Whereas calcification is thought to stabilize coronary plaques against disruption and thrombosis,[22] the question in carotid arteries of whether calcification increases or decreases the risk of subsequent neurologic events, as discussed in a recent review,[5] is controversial. No clinical study, however, has shown a relationship between calcification and vulnerable plaques. Inasmuch as lipid and hemorrhage seem to be the most diagnostically relevant components in a plaque, because they are related to vulnerable plaques and neurologic symptoms,[5] the value of spiral CT scanning in evaluating plaque morphology appears questionable.

In conclusion, spiral CT imaging seems to correlate with the echogenicity of carotid atherosclerotic plaques on B-mode ultrasonography. The spiral CT method, however, is much more complex and demands more resources than B-mode ultrasonographic imaging. Furthermore, because spiral CT imaging predicts only the histologic content of calcification in carotid plaques, it is currently not useful for predicting vulnerable plaques.

References

1. Vallabhajosula S, Fuster V. Atherosclerosis: imaging techniques and the evolving role of nuclear medicine. J Nucl Med 1997; 38:1788–1796.
2. European Carotid Surgery Trialists' Collaborative Group. Randomised trial of endarterectomy for recently symptomatic carotid stenosis: final results of the MRC European Carotid Surgery Trial (ECST). Lancet 1998; 351:1379–1387.
3. Barnett HJM, Taylor DW, Eliasziw M, et al, for the North American Symptomatic Carotid Endarterectomy Trial Collaborators. Benefit of carotid endarterectomy in patients with symptomatic moderate or severe stenosis. New Engl J Med 1998; 339:1415–1425.
4. Falk E. Coronary plaque disruption. Circulation 1995; 92:657–671.
5. Grønholdt M-LM. Ultrasound and lipoproteins as predictors of lipid-rich, rupture-prone plaques in the carotid artery. Arterioscler Thromb Vasc Biol 1999; 19:2–13.
6. Polak JF, Shemanski L, O'Leary DH, et al. Hypoechoic plaque at US of the carotid artery: an independent risk factor for incident stroke in adults aged 65 years or older. Cardiovascular Health Study. Radiology 1998; 208:649–654.

7. Carr S, Farb A, Pearce WH, Virmani R, Yao JST. Atherosclerotic plaque rupture in symptomatic carotid artery stenosis. J Vasc Surg 1996; 23:755–766.
8. Milei J, Parodi JC, Alonso GF, Barone A, Grana D, Matturi L. Carotid rupture and intraplaque hemorrhage: immunophenotype and role of cells involved. Am Heart J 1998; 136:1096–1105.
9. Shinnar M, Fallon JT, Wehrli S, et al. The diagnostic accuracy of ex vivo MRI for human atherosclerotic plaque characterization. Arteriosclerosis 1999; 19:2756–2761.
10. Toussaint JF, LaMuraglia GM, Southern JF, Fuster V, Kantor HL. Magnetic resonance images lipid, fibrous, calcified, hemorrhagic, and thrombotic components of human atherosclerosis in vivo. Circulation 1996; 94:932–938.
11. Hatsukami TS, Ross R, Polissar NL, Yuan C. Visualization of fibrous cap thickness and rupture in human atherosclerotic carotid plaque in vivo with high-resolution magnetic resonance imaging. Circulation 2000; 102:959–964.
12. Streifler JY, Eliasziw M, Fox AJ, et al, for the North American Symptomatic Carotid Endarterectomy Trial. Angiographic detection of carotid plaque ulceration. Comparison with surgical observations in a multicenter study. Stroke 1994; 25:1130–1132.
13. Schroeder TV, Sillesen H, Grønholdt MLM. Carotid endarterectomy without arteriography. J Vasc Invest 1998; 4:5–9.
14. Oliver TB, Lammie GA, Wright AR, et al. Atherosclerotic plaque at the carotid bifurcation: CT angiographic appearance with histopathologic correlation. AJNR Am J Neuroradiol 1999; 20:897–901.
15. Estes JM, Quist WC, Lo Gerfo FW, Costello P. Noninvasive characterization of plaque morphology using helical computed tomography. J Cardiovasc Surg 1998; 39:527–534.
16. Grønholdt M-LM, Wiebe BM, Laursen H, Nielsen TG, Schroeder TV, Sillesen H. Lipid-rich carotid artery plaques may appear echolucent on ultrasound B-mode images and may be associated with intraplaque haemorrhage. Eur J Vasc Endovasc Surg 1997; 14:439–445.
17. Bland JM, Altman DG. Statistical methods for assessing agreement between two methods of clinical measurement. Lancet 1986; 1:307–310.
18. Grønholdt M-LM, Nordestgaard BG, Wiebe BM, Wilhjelm JE, Sillesen H. Echolucency of computerized ultrasound images of carotid atherosclerotic plaques are associated with increased levels of triglyceride-rich lipoproteins as well as increased plaque lipid content. Circulation 1998; 97:34–40.
19. Marks MP, Napel S, Jordan JE, Enzman DR. Diagnosis of carotid artery disease: preliminary experience with maximum-intensity-projection spiral CT angiography. AJR Am J Roentgenol 1993; 160:1267–1271.
20. Picano E, Landini L, Distante A, et al. Angle dependence of ultrasonic backscatter in arterial tissues: a study in vitro. Circulation 1985; 72:572–576.
21. Wilhjelm JE, Grønholdt M-LM, Wiebe B, Jespersen SK, Hansen LK, Sillesen H. Quantitative analysis of ultrasound B-mode images of carotid atherosclerotic plaque: correlation with visual classification and histological examination. IEEE Trans Med Imaging 1998; 17:910–922.
22. Wexler L, Brundage B, Crouse J, et al. Coronary artery calcification: pathophysiology, epidemiology, imaging methods, and clinical implications. Circulation 1996; 94:1175–1192.
23. Agatson AS, Janowitz WR, Hildner FJ, Zusmer NR, Viamonte M Jr, Detrano R. Quantification of coronary artery calcium using ultrafast computed tomography. J Am Coll Cardiol 1990; 15:827–832.
24. Janowitz WR, Agatson AS, Kaplan G, Viamonte M Jr. Differences in prevalence and extent of coronary calcium detected by ultrafast computed tomography in asymptomatic men and women. Am J Cardiol 1993; 72:247–254.